

## Modification of spatiotemporal pattern formation in an excitable medium by continuous variation of its intrinsic parameters: CO oxidation on Pt(110)

K. Asakura, J. Lauterbach, H. H. Rotermund, and G. Ertl

*Fritz-Haber-Institut der Max-Planck-Gesellschaft, Faradayweg 4-6, D-14195 Berlin (Dahlem), Germany*

(Received 17 June 1994)

The phenomenology of spatiotemporal concentration patterns associated with the catalytic oxidation of CO on a Pt(110) surface for conditions of excitability as monitored by photoemission electron microscopy is affected by deposition of submonolayer quantities of Au. This is due to continuous variation of the intrinsic kinetic parameters while the degree of homogeneity of the medium on the mesoscopic scale remains unaltered.

The development of spatiotemporal concentration patterns on single-crystal surfaces, formed in the course of a catalytic reaction by the chemisorbed species involved, has been investigated extensively during the past few years.<sup>1</sup> The most frequently studied system has been the oxidation of carbon monoxide on Pt(110), whereby patterns with typical length scales on the  $\mu\text{m}$  range were imaged by photoemission electron microscopy (PEEM), a technique whose contrast is based on local differences of the work function associated with varying adsorbate concentrations. A wide scenario of patterns could be identified with this system, ranging from propagating wave fronts, spiral waves, solitary-type waves to oscillating target patterns, standing waves, and chaotic behavior ("chemical turbulence").<sup>2,3</sup> Successful theoretical modeling of a large fraction of these phenomena could be achieved by solution of the partial reaction-diffusion equations modeling the underlying reaction steps.<sup>4-7</sup>

The properties of the concentration patterns are thereafter governed by the rate parameters, such as sticking coefficients, diffusion constants, etc., formulated within a continuum-model description and averaged over *mesoscopic* length scales as relevant for the pattern formation. The validity of this concept was checked in the present work through modification of these parameters by deposition of small quantities (far below submonolayer) of an inert material (gold) onto the active Pt(110) surface. This approach enabled investigation of pattern formation in an excitable medium with continuous variation of the intrinsic properties and lead, in addition, to the emergence of effects which are attributed to the gradual breakdown of spatial uniformity. Au atoms evaporated onto a Pt(110) surface form, at low coverages, a randomly dispersed overlayer which inhibits locally CO as well as O<sub>2</sub> absorption, but does not noticeably affect the properties of neighboring Pt atoms. In addition, diffusion into the bulk becomes appreciable only at temperatures beyond  $\sim 850$  K.<sup>8,9</sup>

The experiments were performed in a UHV system equipped with a photoemission electron microscope<sup>10</sup> and standard facilities for surface preparation and characterization. The Pt(110) sample was cleaned by repeated cycles of oxidation at 800 K, Ar<sup>+</sup>-ion sputtering, and annealing at 1000 K. Au was evaporated from a resistively

heated, gold-coated tungsten wire, whereby the deposition rate was monitored by a quartz microbalance. The concentration of Au atoms blocking sites on the Pt(110) surface was determined through the total takeup of CO as monitored by subsequent thermal-desorption spectroscopy, assuming that a monolayer (1 ML) of Au completely inhibits CO adsorption above room temperature.<sup>9</sup> The work function  $\phi$  of the clean Pt(110) surface is slightly higher than if covered with Au.<sup>11</sup>  $\phi$  increases by CO adsorption and even more by the presence of chemisorbed O atoms. Hence O-covered regions appear dark and CO-covered patches are gray in the PEEM images to be presented.

In the following we shall focus on situations under which the surface is in an excitable state in which propagating concentration patterns may form. The properties of a pure Pt(110) surface in this regime have been investigated before in detail.<sup>3</sup> If for a fixed set of temperature  $T$  and O<sub>2</sub> partial pressure  $p_{\text{O}_2}$  the third control parameter, CO partial pressure  $p_{\text{CO}}$ , is continuously increased, the system passes through a stable state in which the surface is predominantly O covered into an excitable region and finally again into a stable state which is now essentially CO covered. The main features in the excitable regime are propagating reaction-diffusion fronts, spiral waves, and (in a very limited range of parameters) solitary waves.<sup>3</sup>

If the Pt(110) surface was covered with gold, increasing Au concentrations were found to decrease the lower CO pressure limit for the transition into the excitable state. For Au coverages exceeding  $\theta_{\text{Au}} > 0.3$  formation of patterns was no longer observed; the surface was then even for low  $p_{\text{CO}}$  predominantly covered by adsorbed CO and the reactivity was very low.

This effect has to be attributed to the fact that dissociative chemisorption of oxygen is more strongly affected by the presence of gold than adsorption of CO. In the latter case, the inert Au atoms essentially reduce the available area for adsorption, while for oxygen dissociation a larger ensemble of neighboring Pt atoms is required whose concentration drops much stronger than linearly with  $\theta_{\text{Au}}$ . Since the transition from the O-covered to the excitable range is governed by the balance between  $\theta_{\text{O}}$  and  $\theta_{\text{CO}}$ , in

the presence of Au the critical balance will be reached at lower  $p_{\text{CO}}$ .

Figure 1 shows a PEEM image from a Pt(110) surface on which only the lower part was covered by  $\theta_{\text{Au}}=0.3$ . The reaction conditions were chosen in a way that the pure Pt(110) surface is in a stable, mainly O-covered state, i.e.,  $p_{\text{CO}}$  is just below the critical value for transition into the excitable regime. The Au-covered part, however, strongly inhibits oxygen adsorption and is hence predominantly occupied by adsorbed CO as reflected by the higher brightness (equal to the lower work function in the PEEM image). Interestingly, this region may trigger CO concentration waves across the boundary to the pure Pt(110) area where they propagate up to several tenths of a mm as becomes evident from the sequence of images in Fig. 1. This example demonstrates how the reactivity of a surface may be affected on mesoscopic length scales by adjacent areas with different reaction properties. Similar effects had been observed previously with pure Pt samples exhibiting varying surface structure, either on a cylindrical single crystal<sup>12</sup> or on a tip imaged by field ion microscopy, serving as model for small catalyst particles.<sup>13</sup>

An Au-covered area of limited dimensions may act as core for spiral waves. This becomes evident from inspection of Fig. 2, where a patch with  $\sim 0.4$  mm diameter covered by 0.2 ML Au is essentially covered by adsorbed CO, while the surrounding Pt area is in the excitable state. A multiarmed oxygen-covered spiral wave is emanating from the extended core formed by the Au-covered region, similarly as in previous experiments where a defect zone of comparable size was created on the Pt surface by an intense laser beam.<sup>3</sup> In the present example the widths of the oxygen spiral arms grow with increasing distance from the core so that the CO-covered areas in between shrink. Presumably this effect is influenced by deviation from the steplike concentration profile of gold.

Figure 3 shows an image from two adjacent parts of the surface from which one consists of pure Pt(110) while

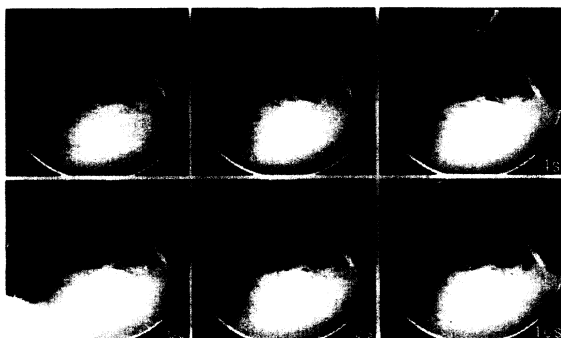


FIG. 1. A sequence of photoemission electron microscopy (PEEM) images (diameter  $500 \mu\text{m}$ ), recorded in intervals of 2 s from a Pt(110) surface whose lower part was covered by 0.3 ML Au and which was exposed to  $4 \times 10^{-4}$  mbar  $\text{O}_2$  and  $2.9 \times 10^{-5}$  mbar CO at 470 K. The Au-containing part is predominantly covered by adsorbed CO and emits continuously CO concentration waves into the gold-free region.

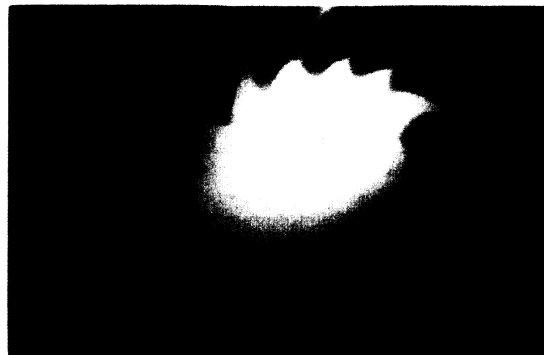


FIG. 2. Around an elliptical region covered by 0.2 ML Au a multiarmed spiral is formed. (Image diameter  $400 \mu\text{m}$ .)  $p_{\text{O}_2} = 4 \times 10^{-4}$  mbar,  $p_{\text{CO}} = 3.3 \times 10^{-5}$  mbar,  $T = 430$  K.

the other one is covered by 0.05 ML Au. Both areas are in the excitable state exhibiting spiral waves. It turns out that on the gold part the spiral wavelength is smaller and front propagation speed is lower. Along the  $(1\bar{1}0)$  direction the corresponding values are  $18 \mu\text{m}$  and  $2.2 \mu\text{m/s}$  on the Au-covered part, and  $32 \mu\text{m}$  and  $2.8 \mu\text{m/s}$  on the pure Pt surface, respectively.

The elliptical shape of the spiral waves is caused by the anisotropy of surface diffusion of adsorbed CO (which is the most mobile surface species).<sup>14</sup> The ellipticity, i.e., the ratio of propagation speeds along the  $(1\bar{1}0)$  and  $(001)$  directions, was found to be identical for both parts of the surface. This means that the deposition of small amounts of Au does not noticeably affect the anisotropy of surface diffusion although the magnitude of the surface diffusion coefficient is altered.

Generally, the propagation speed  $c$  of a chemical wave is determined by  $(kD)^{1/2}$ , where  $k$  is an effective rate constant and  $D$  a diffusion coefficient.<sup>15</sup> Theoretical treatment of the present system in terms of the partial differential equations modeling the reaction steps in-



FIG. 3. Spiral waves on two adjacent sections of the Pt(110) surface from which the left one is covered by 0.05 ML Au.  $p_{\text{O}_2} = 4 \times 10^{-4}$  mbar,  $p_{\text{CO}} = 4.6 \times 10^{-5}$  mbar,  $T = 460$  K.

volved revealed that a good approximation is reached by a formalism in terms of two variables, namely, the CO coverage and the fraction of the surface exhibiting the  $1 \times 1$  structure (which is in turn affected by the CO coverage), while the O coverage is strongly anticorrelated with the CO coverage and can hence be eliminated.<sup>5</sup> The equations become dimensionless if the actual temporal ( $t'$ ) and spatial coordinates ( $r'$ ) are scaled as follows:

$$t = k_5 t', \quad r = (k_5 / D_u)^{1/2} r',$$

$k_5$  is the rate constant for the  $1 \times 1 \rightarrow 1 \times 2$  structural transformation of the Pt(110) surface, and  $D_u$  is the diffusion coefficient for adsorbed CO. Low-energy electron diffraction experiments revealed that  $k_5$  is not noticeably affected by the presence of small quantities of Au so that  $D_u$  is left as the main source for the mentioned differences. Since the adsorption energy for CO on Au is much smaller than on Pt, an Au atom on a Pt surface represents essentially a large potential barrier and hence an obstacle for a migrating CO molecule, and therefore a reduction of the CO diffusion coefficient will be the consequence.

Specifically, since  $r' = (D_u / k_5)^{1/2} r$ , a decrease of  $D_u$  will reduce the actual length for any given solution  $r$ , which accounts for the decrease of spiral width and wavelength in the presence of Au atoms.

In the presence of small quantities of Au the surface exhibits generally a higher density of spiral waves than with pure Pt(110). This becomes, for example, evident from the PEEM images reproduced in Fig. 4 recorded with  $\theta_{\text{Au}} = 0.075$ . Frequently the separation between neighboring spiral cores becomes smaller than the wavelengths of the spirals. As a consequence spirals may break up and eventually transform into closed wave fronts commonly denoted as target patterns. Continuous transitions between spiral and target states were quite recently observed with a system subject to Rayleigh-Bénard convection and it was speculated that these patterns are generated by similar mechanisms,<sup>16</sup> as is supported by the present findings.

With the Belousov-Zhabotinsky reaction, introduction of nucleation centers with diameters up to about 1 mm

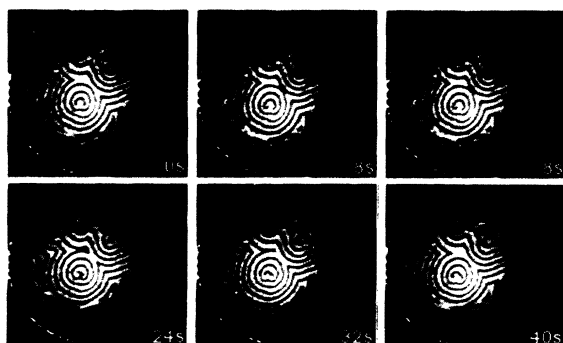


FIG. 4. A sequence of PEEM images (diameter  $300 \mu\text{m}$ ) recorded in intervals of 8 s from a Pt(110) surface covered by 0.075 ML Au.  $p_{\text{O}_2} = 4 \times 10^{-4}$  mbar,  $p_{\text{CO}} = 8 \times 10^{-6}$  mbar,  $T = 400$  K.

had been found to initiate the spontaneous formation of spiral waves and eventually even the formation of irregular patterns due to an overcrowding of spirals.<sup>17</sup> With the present system, the deposition of small concentrations of Au causes an inhomogeneity of the medium on *microscopic* (i.e., atomic) scale which is certainly not directly responsible for the higher density of nucleation centers. Rather on a *mesoscopic* scale the degree of homogeneity of the medium remains unaltered. If we assume random distribution of the Au atoms, then at the low coverages under discussion the average distance between the adatoms (i.e., the scale of microscopic inhomogeneity) is of the order of a few nm, which is far below the resolution limit of the PEEM technique and about three orders of magnitude smaller than the actual size of the nucleation centers which is on the  $\mu\text{m}$  scale as will be outlined in more detail below. If the Au atoms would, on the other hand, agglomerate to patches these could clearly be distinguished in the PEEM images, which was not the case.

Previous investigations with pure Pt(110), both experimentally<sup>3</sup> and theoretically,<sup>7</sup> had revealed that the minimum core size of the spirals is typically of the order of about  $1 \mu\text{m}$ . This is because the propagation speed  $c$  of a concentration wave depends on the radius of curvature  $R$  of its nucleation center as  $c = c_{\text{pl}} - D/R$ , whereby  $c_{\text{pl}}$  is the speed of the corresponding plane wave. Since a pattern may only grow if  $c > 0$ , a critical radius results:  $R_{\text{crit}} = D/c_{\text{pl}}$ . Since  $c_{\text{pl}}$  is proportional to  $D^{1/2}$  (see above), also  $R_{\text{crit}} \propto D^{1/2}$ . Hence any reduction of  $D$  will also decrease  $R_{\text{crit}}$ . As a consequence, smaller defects on the surface will also become available as nucleation centers whose overall density therefore increases. Irregular spiral patterns were also observed with a polycrystalline Pt foil where the (110)-type grains exhibited inherently an enhanced defect density, again giving rise to increased concentration of nucleation centers for spiral waves.<sup>18</sup>

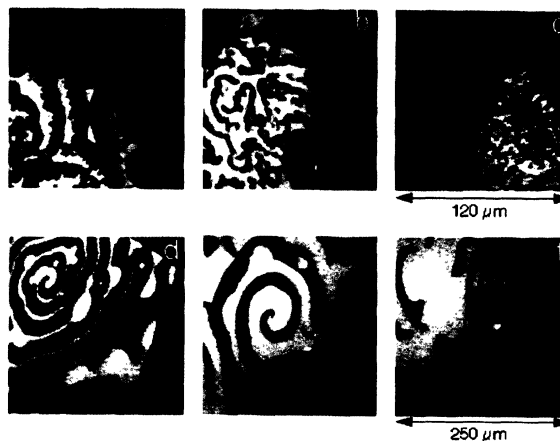


FIG. 5. (a)–(c) PEEM images from a Pt(110) surface covered by 0.1 ML Au exposed at 413 K to  $4 \times 10^{-4}$  mbar  $\text{O}_2$  and varying  $p_{\text{CO}} = 6$  (a), 6.3 (b), and  $7 \times 10^{-6}$  mbar (c). (d)–(f) A similar sequence taken with a bare Pt(110) surface at 413 K,  $p_{\text{O}_2} = 4 \times 10^{-4}$  mbar and  $p_{\text{CO}} = 2.5$  (d), 3.3 (e), and  $4.2 \times 10^{-5}$  mbar (f).

At higher Au coverage (equal to even lower  $D$ ), the accessibility of even further defects as nucleation centers may cause qualitative changes in the patterns. Figures 5(a)–5(c) show a sequence of PEEM images taken at increasing  $p_{\text{CO}}$  with a sample containing  $\theta_{\text{Au}}=0.1$ , with  $p_{\text{O}_2}$  and  $T$  being kept fixed. The wave fronts are no longer sharp, particularly at the rear sides, but become strongly distorted. With increasing CO partial pressure the creation of oxygen waves becomes less and less probable. With pure Pt(110) this causes merely a shrinking of the width of the oxygen waves [see Figs. 5(d)–5(f)]; how-

ever, the fronts are not disrupted and remain sharp. With the Au-covered surface, the increase of the density of nucleation centers eventually causes the appearance of completely disordered and rapidly changing patterns such as in Fig. 5(c), an effect which was never observed with smaller Au concentrations.

The last example demonstrates that continuous variation of the inherent properties of an excitable medium may cause even qualitative variations in its phenomenology of pattern formation. The system presented here is particularly well suited to study such effects.

- 
- <sup>1</sup>G. Ertl, *Adv. Catal.* **37**, 79 (1990); R. Imbihl, *Prog. Surf. Sci.* **44**, 185 (1993); M. Eiswirth and G. Ertl, in *Chemical Waves and Patterns*, edited by K. Showalter and R. Kapral (Kluwer, Amsterdam, in press).
- <sup>2</sup>S. Jakubith, H. H. Rotermund, W. Engel, A. von Oertzen, and G. Ertl, *Phys. Rev. Lett.* **65**, 3013 (1990); H. H. Rotermund, W. Engel, M. Kordesch, and G. Ertl, *Nature* **343**, 355 (1990); H. H. Rotermund, S. Jakubith, A. von Oertzen, and G. Ertl, *Phys. Rev. Lett.* **66**, 3083 (1991).
- <sup>3</sup>S. Nettessheim, A. von Oertzen, H. H. Rotermund, and G. Ertl, *J. Chem. Phys.* **98**, 997 (1993).
- <sup>4</sup>M. Bär, M. Eiswirth, H. H. Rotermund, and G. Ertl, *Phys. Rev. Lett.* **69**, 945 (1992).
- <sup>5</sup>M. Bär, M. Flacke, and M. Eiswirth, *Physica A* **188**, 78 (1992).
- <sup>6</sup>M. Falcke, M. Bär, H. Engel, and M. Eiswirth, *J. Chem. Phys.* **97**, 4555 (1992).
- <sup>7</sup>M. Bär, N. Gottschalk, M. Eiswirth, and G. Ertl, *J. Chem. Phys.* **100**, 1202 (1994).
- <sup>8</sup>J. W. A. Sachtler, M. A. van Hove, J. P. Biberian, and G. A. Somorjai, *Surf. Sci.* **110**, 19 (1981).
- <sup>9</sup>P. W. Davies, M. A. Quinlan, and G. A. Somorjai, *Surf. Sci.* **121**, 290 (1982).
- <sup>10</sup>W. Engel, M. Kordesch, H. H. Rotermund, S. Kubala, and A. von Oertzen, *Ultramicroscopy* **36**, 148 (1991).
- <sup>11</sup>R. Bouwman and W. M. H. Sachtler, *J. Catal.* **19**, 127 (1970).
- <sup>12</sup>M. Sander, R. Imbihl, and G. Ertl, *J. Chem. Phys.* **97**, 5193 (1992).
- <sup>13</sup>V. Gorodetskii, J. Lauterbach, H. H. Rotermund, J. H. Block, and G. Ertl, *Nature* **370**, 276 (1994).
- <sup>14</sup>H. H. Rotermund, S. Nettessheim, A. von Oertzen, and G. Ertl, *Surf. Sci.* **275**, L645 (1992).
- <sup>15</sup>R. Luther, *Z. Elektrochem.* **12**, 596 (1906); R. Arnold, K. Showalter, and J. Tyson, *J. Chem. Educ.* **64**, 740 (1987).
- <sup>16</sup>M. Assenheimer and V. Steinberg, *Nature* **367**, 345 (1994).
- <sup>17</sup>J. Maselko and K. Showalter, *Physica D* **49**, 21 (1991).
- <sup>18</sup>J. Lauterbach, G. Haas, H. H. Rotermund, and G. Ertl, *Surf. Sci.* **294**, 116 (1993).

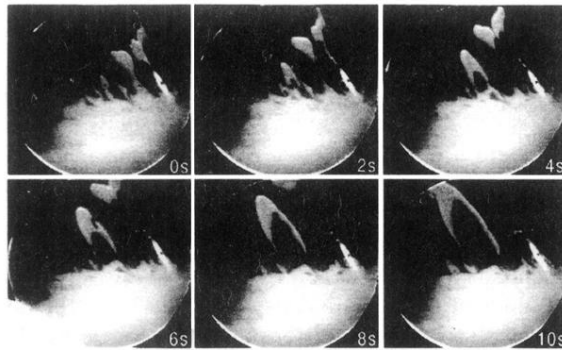


FIG. 1. A sequence of photoemission electron microscopy (PEEM) images (diameter  $500 \mu\text{m}$ ), recorded in intervals of 2 s from a Pt(110) surface whose lower part was covered by 0.3 ML Au and which was exposed to  $4 \times 10^{-4}$  mbar  $\text{O}_2$  and  $2.9 \times 10^{-5}$  mbar CO at 470 K. The Au-containing part is predominantly covered by adsorbed CO and emits continuously CO concentration waves into the gold-free region.

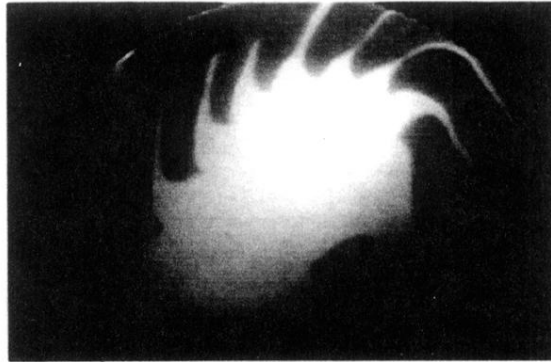


FIG. 2. Around an elliptical region covered by 0.2 ML Au a multiarmed spiral is formed. (Image diameter 400  $\mu\text{m}$ .)  
 $p_{\text{O}_2} = 4 \times 10^{-4}$  mbar,  $p_{\text{CO}} = 3.3 \times 10^{-5}$  mbar,  $T = 430$  K.



FIG. 3. Spiral waves on two adjacent sections of the Pt(110) surface from which the left one is covered by 0.05 ML Au.  $p_{O_2} = 4 \times 10^{-4}$  mbar,  $p_{CO} = 4.6 \times 10^{-5}$  mbar,  $T = 460$  K.

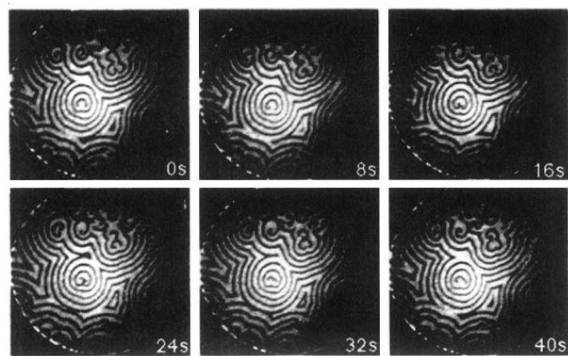


FIG. 4. A sequence of PEEM images (diameter  $300\ \mu\text{m}$ ) recorded in intervals of 8 s from a Pt(110) surface covered by 0.075 ML Au.  $p_{\text{O}_2} = 4 \times 10^{-4}$  mbar,  $p_{\text{CO}} = 8 \times 10^{-6}$  mbar,  $T = 400$  K.



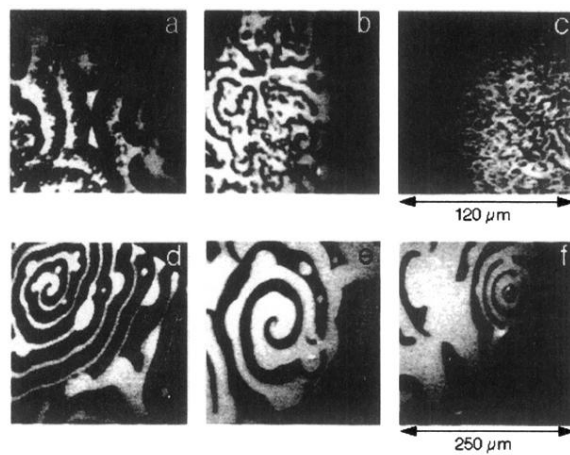


FIG. 5. (a)–(c) PEEM images from a Pt(110) surface covered by 0.1 ML Au exposed at 413 K to  $4 \times 10^{-4}$  mbar  $O_2$  and varying  $p_{CO} = 6$  (a), 6.3 (b), and  $7 \times 10^{-6}$  mbar (c). (d)–(f) A similar sequence taken with a bare Pt(110) surface at 413 K,  $p_{O_2} = 4 \times 10^{-4}$  mbar and  $p_{CO} = 2.5$  (d), 3.3 (e), and  $4.2 \times 10^{-5}$  mbar (f).